REPORT

Synthetic peptides that reproduce the N-terminus of sticholysins as models for the study of their structure-function relationship

Uris Ros, Lohans Pedrera, Diana Martínez, Mayra Tejuca, Fabiola Pazos, Maria E Lanio, ✍ Carlos Alvarez

Centro de Estudio de Proteínas, Facultad de Biología,
Universidad de La Habana, UH
CP 10400, La Habana, Cuba
✍ calvarez@fbio.uh.cu

ABSTRACT

The Caribbean Sea anemone *Stichodactyla helianthus* produces two pore-forming proteins, sticholysins I and II (StI and StII). To clarify the contribution of the first thirty (StII) or thirty-one (StI) N-terminal amino acid residues to the activity of the toxins, four peptides spanning residues 1-31 of StI (StI_{1-31}, StI_{12-31}) and 1-30 of StII ($StII_{1-30}$, $StII_{11-30}$) were synthesized. $StII_{1-30}$ was the most active peptide, followed by StI_{1-31} and the shortest ones. The difference between the hemolytic activities of the largest peptides qualitatively reproduces that found between the respective toxins StI and StII. The results suggest the importance of continuity of the 1-10 hydrophobic amino acid sequence in $StII_{1-30}$ for displaying higher membrane binding and activity. Thus, the different peptide membranotropic action is explained in terms of the differences in their hydrophobic and electrostatic properties. Furthermore, we also demonstrated that $StII_{1-30}$ forms pores of similar radius to that of the protein (around 1 nm), with its N-terminus oriented towards the hydrophobic core of the bilayer while the rest of the peptide is more exposed to the aqueous environment, as hypothesized for sticholysins. Altogether these results demonstrate that synthetic peptides that reproduce sticholysins' N-terminus are not only a good model of these toxins structure and function but, and due to its reduced molecular size, could also be useful biotechnological tools instead of their larger parental proteins. This research won the 2012 Award of the Cuban National Academy of Sciences.

Keywords: sticholysins, *Stichodactyla helianthus*, porins, pore forming peptides

Biotecnología Aplicada 2013;30:312-316

RESUMEN

Péptidos sintéticos que reproducen la secuencia del extremo amino de las sticholysinas como modelos para el estudio de su relación estructura-función. La anémona del mar Caribe *Stichodactyla helianthus* produce dos proteínas formadoras de poros: las sticholysinas I y II (StI y StII). Para dilucidar la contribución de sus primeros 30 (StII) o 31 (StI) aminoácidos del extremo N-terminal a la actividad formadora de poros, se sintetizaron cuatro péptidos que abarcaron los residuos 1 al 31 de StI (StI_{1-31}, StI_{12-31}) y 1 al 30 de StII ($StII_{1-30}$, $StII_{11-30}$). $StII_{1-30}$ fue el más activo, seguido por StI_{1-31}. La diferencia entre las actividades hemolíticas de los péptidos largos reproduce cualitativamente la hallada entre las respectivas toxinas StI y StII. Los resultados sugieren la importancia de la continuidad de la secuencia hidrofóbica 1-10 en el péptido $StII_{1-30}$ para su capacidad de unión a membranas y su actividad. La actividad membranotrópica diferencial de los péptidos se explica por las diferencias en sus propiedades hidrofóbicas y electrostáticas. Además se demostró que $StII_{1-30}$ forma poros con un radio similar a los de la proteína (aproximadamente 1 nm), con su extremo N-terminal hacia el núcleo hidrofóbico de la bicapa lipídica, mientras que el resto está más expuesto hacia el microambiente acuoso, tal como se ha supuesto postulado para las sticholysinas. Ello demuestra que los péptidos sintéticos que reproducen el segmento N-terminal de las sticholysinas son un modelo de la estructura y función de estas toxinas, y herramientas biotecnológicas útiles, sobre la base de su reducido tamaño molecular, a diferencia de sus proteínas nativas de mayor tamaño. Este trabajo mereció el Premio Anual de la Academia de Ciencias de Cuba, 2012.

Palabras clave: sticholysinas, *Stichodactyla helianthus*, porinas, péptidos formadores de poros

*I*ntroduction

The pore-forming proteins sticholysin I and II (StI and StII) produced by the sea anemone *Stichodactyla helianthus* [1] are highly hemolytic toxins with 93 % sequence identity. StI and II form hydrophilic pores both in natural and model lipid membranes of around 1 nm hydrodynamic radius [2]. They belong to the actinoporin family [3], a unique class of eukaryotic pore-forming proteins exclusively found in sea anemones. Actinoporins are cysteine-less proteins, with M_r around 20 kDa and whose putative receptor is sphingomyelin (SM) [4-6]. Despite the extensive work carried out aiming at clarifying how these water-soluble proteins bind, oligomerize, and eventually disrupt target membranes, little is known about the amino acid sequence(s) and/or domains involved in each step of the lytic mechanism [7].

The main difference in the primary sequence between sticholysins lies in their N-terminus, where all the non-conservative substitutions and one conservative substitution are found [8]. When compared to StII, StI contains two additional acidic residues (Glu2 and Asp9) instead of the non- polar amino acid Ala, in positions 1 and 8 of StII and also an extra polar residue (Ser) at position 1; therefore StII's N-terminus

✍ Corresponding author

1. Lanio ME, Morera V, Alvarez C, Tejuca M, Gomez T, Pazos F, *et al*. Purification and characterization of two hemolysins from *Stichodactyla helianthus*. Toxicon. 2001;39(2-3):187-94.

2. Tejuca M, Dalla Serra M, Potrich C, Alvarez C, Menestrina G. Sizing the radius of the pore formed in erythrocytes and lipid vesicles by the toxin sticholysin I from the sea anemone *Stichodactyla helianthus*. J Membr Biol. 2001;183(2):125-35.

is more hydrophobic than its counterpart in StI. The most noteworthy functional difference between StI and StII is that the lytic activity of StII is approximately 3-6 fold higher than that of StI [9]. Since the N-terminal region of the toxins is probably involved in pore formation [10], their different hemolytic activity could be due, at least partly, to differences in this region [9].

To gain insight into the molecular mechanism of the differential activity of sticholysins, peptides reproducing the N-terminal region of StI residues 1-31 (StI_{1-31}: SELAGTIIDGASLTFEVLDKVLGELGKV SRK) and 12-31 (StI_{12-31}: SLTFEVLDKVLGELGKV SRK) as well as StII residues 1-30 ($StII_{1-30}$: ALAGT IIAGASLTFQVLDKVLEELGKVSRK) and 11-30 ($StII_{11-30}$: SLTFQVLDKVLEELGKVSRK) were synthesized. The longest fragments, StI_{1-31}, and $StII_{1-30}$, contain the amphipathic α-helix (residues 14-23) described for StII, preceded by a highly hydrophobic amino acid sequence [10, 11]. Peptides StI_{12-31} and $StII_{11-30}$ lack most of this hydrophobic sequence. All peptides are cationic at pH 7 (net charge +2), except for StI_{1-31} which has no net charge. In this study the peptides conformational and functional properties were analyzed in order to validate them as a model for the study of sticholysins' mechanism of action. Overall, the results here presented demonstrate that studies with synthetic peptides can be useful in the analysis of the contribution of the N-terminus to the activity of sticholysins in order to understand the molecular details of their structure-function relationships for these and other actinoporins.

Materials and methods

Peptide synthesis

The peptides (with amidated C-terminus) were synthesized manually according to the standard N_{α}-Fmoc protecting-group strategy [12] as previously described [13]. The peptides' homogeneity was checked by analytical HPLC (Varian, Walnut Creek, CA, USA), using UV detection at 220 nm. The identity of the peptides was confirmed by electrospray mass spectrometry on a ZMD model apparatus (Micromass, Manchester, UK) and amino acid analysis (Shimadzu model LC-10A/C-47A, Tokyo, Japan).

Circular dichroism studies in solution and in the presence of small unilamellar vesicles

Far UV circular dichroism (CD) spectra were acquired in 0.5 or 1.0 mm path length cuvettes, at room temperature (22 ± 2 °C) using a Jobin Yvon CD6 spectropolarimeter (Longjumeau, France). The instrument was routinely calibrated with an aqueous solution of recrystallized D-10-camphorsulfonic acid. For experiments in the presence of small unilamellar vesicles (SUV), lipid films of phosphatidyl choline:sphingomyelin:phosphatidic acid:cholesterol (PC:SM:PA:Chol; 60:15:5:20) were prepared by evaporation of stock chloroform solutions using a stream of wet nitrogen and submitted to vacuum for not less than 2 h. Multilamellar vesicles (MLV) were obtained by subsequent hydration with buffer. SUV were prepared by thorough sonication of MLV with an ultrasonicator (Branson 450, Danbury, USA) until a clear suspension was obtained. CD spectra of SUV acquired in the absence of peptides were used for baseline correction.

Surface pressure measurements on lipid monolayers

Surface pressure (π) measurements were carried out with a μThrough-S system (Kibron, Helsinki, Finland) at room temperature (22 ± 2 °C) under constant stirring employing plates of ca. 3.14 cm^2. The aqueous phase consisted of 300 μL of Tris-buffered saline (TBS; 145 mM NaCl, 10 mM Tris–HCl, pH 7.4). The lipid mixture was dissolved in chloroform: methanol (2:1, v:v) and was gently spread over the surface; the desired initial surface pressure (π_0) was attained by changing the amount of lipid mixture (PC:SM:PA:Chol, 30:45:5:20) applied to the air-water interface. The peptides were injected into the subphase to achieve 0.1 μM final concentration; at this concentration the peptides have no effect on surface tension of the air-water interface.

Assay of leakage from carboxyfluorescein-containing vesicles

Large unilamellar vesicles (LUV) permeabilization was determined at room temperature (22 ± 2 °C) using a FLUOstar OPTIMA microplate reader (BMG Labtech, Offenburg, Germany) by measuring the fluorescence of released carboxyfluorescein (CF; λ_{exc} = 490 nm and λ_{em} = 520 nm). Peptide samples were two-fold serially diluted in black plastic 96-well microplates (SPL-Life Sciences, Seoul, South Korea) in a final volume of 100 μL of TBS. The reaction was started by adding the same volume of liposomes (10 μM final lipid concentration). After mixing vesicles and peptides, the release of CF into the external medium produced an increase in fluorescence (f) due to dequenching of the dye's fluorescence resulting from dilution. The increase in fluorescence was recorded as a function of time. Maximum release was obtained by adding 0.1 % Triton X-100 (final concentration).

Hemolytic activity

Hemolytic activity was evaluated turbidimetrically at 600 nm at room temperature (22 ± 2 °C) in a Labsystems microplate reader (Helsinki, Finland). Erythrocyte suspension was prepared using pooled fresh human red blood cells collected intravenously from at least four healthy volunteers. Cells were washed by repeated centrifugation (600 *g*, 15 min) and the cell pellet resuspended in TBS and finally diluted to an apparent absorbance of 0.1 at 600 nm. Peptide samples in 100 μL of TBS were two-fold serially diluted in a flat-bottom 96-well microplate. The reaction was started by adding the same volume of red blood cells (200 μL total volume). The decrease in apparent absorbance was recorded as a function of time with intermittent shaking.

Pore size determination

Pore size was determined in human red blood cells following the hemolytic assay described in the previous section. Briefly, in each well, a fixed concentration (20 or 160 μM) of $StII_{1-30}$ was present, in a final

3. Kem WR. Sea anemones toxins: structure and action. In: Hessinger DA, Lenhoff HM, editors. The biology of nematocysts. San Diego: Academic Press; 1988. p. 375-405.

4. Tejuca M, Serra MD, Ferreras M, Lanio ME, Menestrina G. Mechanism of membrane permeabilization by sticholysin I, a cytolysin isolated from the venom of the sea anemone *Stichodactyla helianthus*. Biochemistry. 1996;35(47):14947-57.

5. Valcarcel CA, Dalla Serra M, Potrich C, Bernhart I, Tejuca M, Martinez D, *et al*. Effects of lipid composition on membrane permeabilization by sticholysin I and II, two cytolysins of the sea anemone *Stichodactyla helianthus*. Biophys J. 2001;80(6):2761-74.

6. Anderluh G, Macek P. Cytolytic peptide and protein toxins from sea anemones (Anthozoa: Actiniaria). Toxicon. 2002;40(2):111-24.

7. Alvarez C, Mancheño JM, Martinez D, Tejuca M, Pazos F, Lanio ME. Sticholysins, two pore-forming toxins produced by the Caribbean Sea anemone *Stichodactyla helianthus*: their interaction with membranes. Toxicon. 2009;54(8):1135-47.

8. Huerta V, Morera V, Guanche Y, Chinea G, Gonzalez LJ, Betancourt L, *et al*. Primary structure of two cytolysin isoforms from Stichodactyla helianthus differing in their hemolytic activity. Toxicon. 2001; 39(8):1253-6.

9. Martinez D, Campos AM, Pazos F, Alvarez C, Lanio ME, Casallanovo F, *et al*. Properties of St I and St II, two isotoxins isolated from *Stichodactyla helianthus*: a comparison. Toxicon. 2001;39(10):1547-60.

10. Mancheño JM, Martin-Benito J, Martinez-Ripoll M, Gavilanes JG, Hermoso JA. Crystal and electron microscopy structures of sticholysin II actinoporin reveal insights into the mechanism of membrane pore formation. Structure. 2003;11(11):1319-28.

11. Castrillo I, Alegre-Cebollada J, Martínez del Pozo A, Gavilanes JG, Santoro J, Bruix M. 1H, 13C, and 15N NMR assignments of the actinoporin Sticholysin I. Biomol NMR Assign. 2009;3(1):5-7.

12. Atherton E, Sheppard RC. Solid phase peptide synthesis: A practical approach; Oxford: Oxford University Press; 1989.

13. Casallanovo F, de Oliveira FJ, de Souza FC, Ros U, Martinez Y, Penton D, *et al*. Model peptides mimic the structure and function of the N-terminus of the pore-forming toxin sticholysin II. Biopolymers. 2006;84(2):169-80.

volume of 100 µL of TBS, with or without 60 mM of one member of the polyethylene glycol series (PEG, with their hydrated radii in parentheses): PEG200 (0.40 nm), PEG400 (0.56 nm), PEG600, (0.69 nm), PEG900 (0.85 nm), PEG1000 (0.89 nm), PEG1500 (1.1 nm), PEG2000 (1.27 nm), and PEG3000 (1.4 nm). Addition of large osmoticants increased the half-time of peptide-induced hemolysis (t½), in a size-dependent manner. The difference t½ – t½^o, the half-times in the presence and absence of osmotic protectants, respectively, was used as an estimate of the induced delay. This parameter measures the time necessary for an osmolite to diffuse inside the cell through the toxin-induced lesions. Accordingly, 1/(t½ – t½^o) is an estimate of the PEG permeability through the pore, which is inversely related to the PEG size. Thus, dividing the data by the permeability of a reference polymer (in this case, PEG200) the dependence of the relative permeability of the molecules versus their size was fitted to a Renkin plot [14]; which allowed estimating the radii of the pores formed by $StII_{1-30}$.

Fluorescence assays with Trp-containing peptides analogs of $StII_{1-30}$

Binding of Trp-peptides to SUV was followed by the increase in Trp fluorescence. Fluorescence measurements were carried out at room temperature (22 ± 2 ^{o}C) in a spectrofluorimeter (Hitachi, F-4500, Tokyo, Japan) using quartz cuvettes with excitation and emission slits of 5 and 10 nm, respectively. The samples were excited at 280 nm and the emission spectra were recorded from 300 to 440 nm. Increasing amounts of SUV were added to the peptide in milliQ water adjusted to pH 7.4, and the spectrum was recorded for each lipidic concentration. Corrections were made for sample dilution and for light scattering caused by the vesicles.

Quenching of Trp intrinsic fluorescence by acrylamide

Trp quenching was achieved by adding the water-soluble quencher acrylamide in the presence of SUV. Acrylamide quenching experiments were carried out using 20 µM of peptide and 400 µM of total lipid. Samples were prepared in MilliQ water adjusted to pH 7.4; excited at 280 nm and the emission spectra were recorded from 300 to 440 nm after addition of acrylamide (up to 0.25 mM). Spectral correction was made by subtracting spectra measured under identical conditions but without the peptide. The experimental data were analyzed according to the Stern-Volmer equation [15].

Results and discussion

StI and StII are characterized by a few amino acid substitutions (up to 13) spread throughout the primary sequence, with the non-conservative changes in the first thirty amino acid residues of their N-termini [8]. In fact, this is the most variable sequence in these and other actinoporins [6]. The presence of a hydrophobic sequence (approximately residues 1-10) preceding a highly amphipathic (approximately residues 14-35) sequence both in StI and StII N-termini supports the assumption that this region is probably involved in pore-formation [10].

In this study, the conformational and functional properties of synthetic peptides derived from StI (StI_{1-31} and StI_{12-31}) were characterized and compared with those of their homologues of StII ($StII_{1-30}$ and $StII_{11-30}$). The conformational properties of the four peptides in solution were assessed, upon binding to model membranes, and permeabilization activity in vesicles and red blood cells aiming at clarifying their relative contribution to the pore-forming activity of the toxins.

In solution all peptides remained essentially structure-less as indicated by the presence of a negative band centered near 200 nm in the corresponding CD spectra. The more or less pronounced shoulder around 222 nm would be indicating that at least another population coexists with certain degree of secondary structure. Remarkably, $StII_{1-30}$ has a higher tendency to acquire secondary structure and/or aggregate in solution. For this peptide the ratio $[\theta]_{222}/[\theta]_{208}$ calculated from CD spectra is higher than 1 (1.14) at 20 µM probably reflecting the formation of interacting coiled-coil helices associated with peptide aggregation [16]. The differences in peptide hydrophobicity might be conditioning their different aggregation and folding in solution.

It was also studied for the first time the conformational changes undergone by the four peptides upon binding to vesicles as model membrane systems. Table shows the number of amino acid residues folded in α-helix in solution and after binding to vesicles. Upon binding to vesicles all peptides increased the content of this secondary structure, although the longest peptides acquired a similar content of α-helical conformation, higher than the shortest ones. These results point out: 1) the important role of the hydrophobic stretch to enhance peptides folding in a membrane mimetic environment and 2) the equivalent potential of both longest peptides to adopt α-helical conformation. We have previously shown that binding of StII to model membranes results in small changes in the toxin's secondary structure [17]. Moreover, FTIR data indicated a 5 % increase in StII α-helical content upon lipid binding. Such an increase corresponds to approximately 9 residues (the protein has 175 amino acids). We suggest that the ca. 16 residues of the longer peptides found in α-helical conformation in SUV might consist of the F14-E23 stretch found in the toxin's X-ray structure [10] plus 6 additional residues. For the shortest peptides approximately 7 residues appear folded in α-helix in SUV. Thus, the lack of the first 10 or 11 residues in $StII_{11-30}$ or StI_{12-31}, respectively, could account for its significantly lower α-helical content, evincing the importance of the N-terminus for helix

14. Renkin EM. Filtration, diffusion, and molecular sieving through porous cellulose membranes. J Gen Physiol. 1954; 38(2):225-43.

15. Lakowicz JR. Principles of Fluorescence Spectroscopy. 3rd ed. New York: Springer; 2006.

16. Lau SY, Taneja AK, Hodges RS. Synthesis of a model protein of defined secondary and quaternary structure. Effect of chain length on the stabilization and formation of two-stranded alpha-helical coiled-coils. J Biol Chem. 1984;259(21):13253-61.

17. Menestrina G, Cabiaux V, Tejuca M. Secondary structure of sea anemone cytolysins in soluble and membrane bound form by infrared spectroscopy. Biochem Biophys Res Commun. 1999;254(1):174-80.

Table. Parameters derived from peptides' functional and conformational characterization

Peptide	aa α helix in solution (No.)	aa α helix in SUV (No.)	π_c (mN/m)	C_{15} (µM)	HC_{15} (µM)
$StII_{1-30}$	3	16	44	0.45	10
$StII_{11-30}$	2	7	40	50	20
StI_{1-31}	2	16	36	13	20
StI_{12-31}	2	7	41	50	20

aa α helix in solution: amino acid residues folded in α-helix in solution.
aa α helix in SUV: amino acid residues folded in α-helix after binding to small unilamellar vesicles.
π_c: the minimal pressure that must be applied to avoid peptide incorporation into the monolayer.
C_{15}: peptide concentration necessary to permeabilize 15 % of the vesicles.
HC_{15}: peptide concentration necessary to cause the hemolysis of 15 % of red blood cells.

increment and stabilization.

In addition, we studied binding of peptides to monolayers as membrane mimetic systems. It is remarkable that all peptides attained π_c values higher than 35 mN/m (Table), indicating that they probably penetrate this lipid monolayer [18]. This value for $StII_{1-30}$ was higher than that for StI_{1-31}. The presence of phosphatidic acid might enhance $StII_{1-30}$ binding by promoting a larger interaction to this negatively charged monolayer, a fact that points out a possible role of peptides' charge on their binding to membranes. Noteworthy, when StI_{1-31} was devoid of the first N-terminal 11 amino acids, the truncated peptide StI_{12-31} yielded a higher π_c in the negatively charged monolayer (Table). These results clearly indicate that the first sequence of StI carrying the two extra anionic residues (Glu2 and Asp9) somehow hinders binding to the negatively charged membrane, under the experimental conditions.

Whether the peptides were able to permeabilize LUV and promote lysis of human red blood cells were also examined. Peptides' activity was in the micromolar concentration range (Table) for all peptides in contrast to the proteins, whose activity is in the nanomolar range [9]. The requirement of much higher peptide concentration than that of the protein is probably due to the fact that other protein regions also play a role in the toxins' activity. In this context, it should be noted that the peptides lack the phosphocholine binding site located in a region rich in aromatic amino acids, highly conserved in the actinoporin family, which is proposed to mediate the initial attachment to membranes [10]. The fact that the peptides' activity resides in the micromolar concentration range, in contrast to the toxins' activity (in the nanomolar range [9]), emphasizes the importance of the rest of the protein for activity even if it does not participate in pore lining.

Moreover, while $StII_{1-30}$ promoted a distinguishably larger effect, the activity for the remaining of the peptides was lower. This result is in good agreement with the higher lytic activity of StII when compared with StI [9]. The activity of all short peptides, derived from both StI (StI_{12-31}) and StII ($StII_{11-30}$), is low and similar. Furthermore, different from what happens in the case of the peptides derived from StII the sequence encompassing the first eleven residues in StI_{1-31} does not enhance its functional activity. In fact, when the average hydrophobicity per residue is calculated using the Kyte-Doolittle scale [19], the first 14 residues of StII yield a value of 1.68, while the first 15 residues of StI results in 0.81, supporting the notion that the higher hydrophobicity of the first residues of StII are decisive for a proper anchoring of the N-terminus to the membrane.

In view of the higher ability of $StII_{1-30}$ to mimic StII and to lyse red blood cells, we decided to estimate the size of the lesion in the membrane, taking advantage of the colloid-osmotic characteristics of StII-induced hemolysis. The method was essentially the same previously used to estimate the radii of the pores formed by sticholysins [2] from the Renkin plot [14] (Figure A) which provided an estimate of the pore radius of 0.98 and 0.94 nm for the experimental values obtained for 20 and 160 μM, respectively. The similarity of the values obtained for both concentrations could mean,

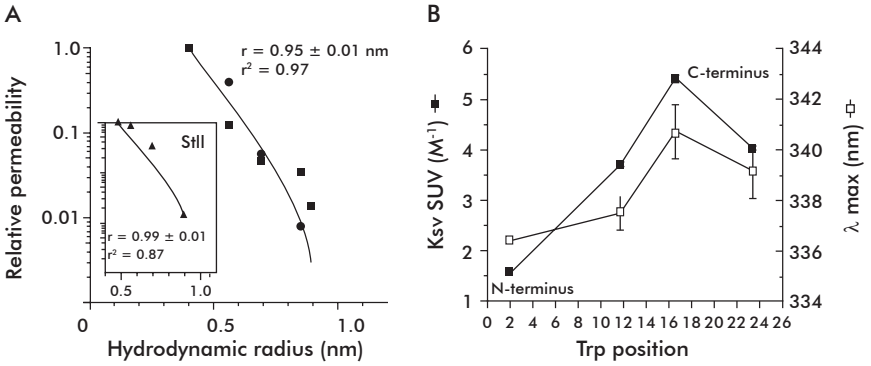

Figure. Size and orientation of the pore formed by $StII_{1-30}$ in membrane. A) Radius of the pore formed by $StII_{1-30}$ in human red blood cells estimated by the Renkin's plot. The solid line is the best fit of the Renkin equation for all experimental values obtained (squares and circles correspond to 20 and 160 μM $StII_{1-30}$, respectively). r: hydrodynamic radius (nm); r^2: determination coefficient. B) $StII_{1-30}$ orientation in membrane. Values of Ksv and λmax obtained from the fluorescence properties of Trp-containing peptides analogs of $StII_{1-30}$ in the presence of SUV. Ksv: Stern-Volmer constant obtained from acrylamide quenching assays. Trp peptides analogues: $StII_{1-30L2W}$, $StII_{1-30L12W}$, $StII_{1-30L17W}$, and $StII_{1-30L24W}$.

as was demonstrated for StII, that the lesion radius is independent of toxin concentration and consequently, has a fixed peptide predominant structure. Figure A shows the experimental values obtained in both series of experiments and the best fit of the Renkin equation for the data. This fit yielded a radius of 0.95 ± 0.01 nm, a value similar to that found for StII under the same experimental conditions (0.99 nm; Figure A, inset).

Trp fluorescence is a useful tool to study binding of proteins and peptides to membranes by sensing changes in their local environment. Here, Trp-analogs of $StII_{1-30}$ ($StII_{1-30L2W}$, $StII_{1-30L12W}$, $StII_{1-30L17W}$, $StII_{1-30L24W}$) were used to determine their orientation in SUV as membrane mimetic systems. For this purpose, peptide-lipid interactions were monitored by following the changes in Trp fluorescence emission spectra of the peptides upon addition of SUV. The values of λmax, obtained from typical fluorescence spectra of peptides and Stern-Volmer (Ksv) values, obtained in the presence of liposomes (Figure B) shows that Trp fluorescence of the peptides behave differently upon binding to membranes. While $StII_{1-30L2W}$ and $StII_{1-30L12W}$ exhibit the lowest λmax (336 nm and 337 nm, respectively), these values are 341 nm and 339 nm for $StII_{1-30L17W}$ and $StII_{1-30L24W}$, respectively. In agreement with these observations, $StII_{1-30L2W}$ exhibits the lowest Ksv value for acrylamide quenching, followed by $StII_{1-30L12W}$. The smaller values of λmax and Ksv obtained for $StII_{1-30L2W}$ evinces that Trp2 is most deeply buried into the membrane. Conversely, Trp residues in $StII_{1-30L12W}$, $StII_{1-30L17W}$, and $StII_{1-30L24W}$ are more exposed to the water-lipid interface. This piece of evidence supports the idea that $StII_{1-30}$ is oriented in bilayers with the N-terminus in the direction of the membrane hydrophobic core and the C-terminus towards the water-lipid interface.

Concluding remarks

The present results provide a clear demonstration of the role of the N-terminal segment of actinoporins in pore formation. In particular, the results stress the contribution of the hydrophobic segment to the differential St's activity. This contribution is the first

18. Brockman H. Lipid monolayers: why use half a membrane to characterize protein-membrane interactions? Curr Opin Struct Biol. 1999;9:438-43.

19. Kyte J, Doolittle RF. A simple method for displaying the hydropathic character of a protein. J Mol Biol. 1982;157(1):105-32.

report of a model 3 kDa peptide that can reproduce the pore-forming activity of an actinoporin (20 kDa), and opens a new approach for the study of these proteins, namely, the use of smaller molecules that mimic their function. Furthermore, the synthetic peptide $StII_{1-30}$ is not only a good model of StII structure and function but, due to its reduced molecular size, could also be useful as a biotechnological tool. Studies of the interaction of this peptide and properly engineered analogues with biological and model membranes should provide insight into the molecular details of the mechanism of peptide-membrane interaction and should allow the optimization of their potential applications.